

ORIGINAL ARTICLE

Tensile Characteristics of Low Density Infill Patterns for Mass Reduction of 3D Printed Polylactic Parts

M. N. F. Saniman^{1*}, M. H. M Hashim¹, K. A. Mohammad¹, K. A. Abd Wahid¹, W. M. Wan Muhamad¹ and N. H. Noor Mohamed²

¹Mechanical Engineering Section, Universiti Kuala Lumpur Malaysia France Institute, 43650 Bangi, Selangor, Malaysia

²Department of Mechanical and Manufacturing Engineering, Universiti Malaysia Sarawak, 94300 Kota Samarahan, Sarawak.

ABSTRACT – Various infill patterns are introduced in 3D printing to generate low density objects that leads to reduced cost and fabrication time through mass reduction. However, as a trade-off, the strength of the 3D printed component is uncertain. Confusions arise in determining the infill pattern with highest value of tensile strength since most studies limited only to rectilinear, honeycomb, and concentric infill patterns. As consequences, there are very little information on rarely used infill patterns such as Hilbert curve, Archimedean cord and octagram spiral. Therefore, the purpose of this research is to investigate and compare the tensile strength and strain of all infill patterns in mass reduction of 3D printed components experimentally. Following ASTM D638 type III standard, ten tensile test specimens of each infill patterns with 20% density were printed with an FFF 3D printer and were then tested. It was found that Archimedean cords infill pattern had the highest specific tensile strength of 33.23×10^3 MPa·mm³/g which made it as the optimum infill pattern for the mass reduction of 3D printed parts with a high tensile strength. On the other hand, having the highest specific tensile strain of 18.21×10^3 %·mm³/g, concentric infill pattern was found to be more suitable for producing lightweight parts with a higher elongation before break. Additionally, Hilbert curve infill was the worst selection for mass reduction since it had the lowest values of specific tensile strength and specific strain of 19.80×10^3 MPa·mm³/g and 8.34 %·mm³/g, respectively. Nevertheless, the trends of tensile strength and strain of all six infill patterns had been obtained, especially for rarely investigated infill patterns of Archimedean cords, octagram spiral, and Hilbert curve. Specifically, the trend from the strongest to the weakest (in % compared to solid) for specific tensile strength is rectilinear (38.57%), Archimedean chords (37.29%), concentric (36.57%), octagram spiral (34.79%), honeycomb (27.84%), and Hilbert curve (22.25%), while for specific strain is concentric (102.6%), octagram spiral (83.94%), rectilinear (78.22%), Archimedean cords (77.99%), honeycomb (54.84%), and Hilbert curve (45.14%).

ARTICLE HISTORY

Revised: 24th Mar 2020

Accepted: 25th Apr 2020

KEYWORDS

3D printing;

Mass reduction;

Infill pattern;

Tensile strength, Strain

INTRODUCTION

Fused Filament Fabrication (FFF) based three dimensional (3D) printing, which has been developed in 1980s, is a kind of manufacturing process to produce a three-dimensional products layer by layer [1]. For years, FFF 3D printers were used only by industries. The first at-home personal desktop 3D printer emerged in 2005, which allow individuals to experiment with various innovative product design as well as to create successful prototypes prior to actual manufacturing processes. For example, prototypes of hydrokinetic turbine blade [2], recirculation channel of turbocharger compressor [3], and Eddy current testing probe [4] could be produced via 3D printer based on the conducted numerical simulations and composed design in order to study its manufacturability and producibility [5]. It is due to the fact that 3D printing is generally faster, affordable and easier to use compared to other quick prototyping technologies. This technology also has increased the scholastic and industrial spirits of masses owing to its ability to create complex geometry with customizable material properties [6]. Since the outputs from 3D printers are highly customizable, users' interest in unique products may affect their likelihood to further adopt the current technology, which will only push the technology forward [7].

In product innovation, one of the purposes of using 3D printing technology is to reduce the amount of material used to fabricate any components. In consequences, not only the cost for production could be reduced, but also speeding up the overall manufacturing processes [8]. However, in order to produce the desired lightweight products, all related parameters in 3D printing must be considered such as the type of thermoplastic materials, structural parameters, 3D printing machine parameters, and build support parameters [9-11]. Sood, Ohdar and Mahaprata [12] investigated on layer thickness, printing orientation, raster angle, raster width and air gap while Moscato et. al. [13] studied the effect of various infill density to the mechanical and electrical properties of 3D printed materials. It is noted that there are more than one hundred printing parameters combined, which could affect the tensile strength of 3D printed parts. However, this study focused specifically on the infill patterns, since the selection of infill patterns affect directly with the parameters related to mass reduction such as weight and material usage.

Infill pattern represent the structure printed inside the object. There are several types of infill patterns available such as rectilinear, concentric, honeycomb, octagram spiral, Archimedean chords, and Hilbert curve as shown in Figure 1. Each of these infill patterns have their own characteristics. De Vos, Torah and Tudor [14] stated that rectilinear at 50% infill density is the fastest type of infill pattern to achieve full coverage printing. However, finishing quality of the 3D printed surface was not uniform as some side was thicker than other side. According to Fernandez-Vicente et. al. [15], honeycomb infill pattern could provide a good tensile strength compared to other patterns with slight percentage of difference.

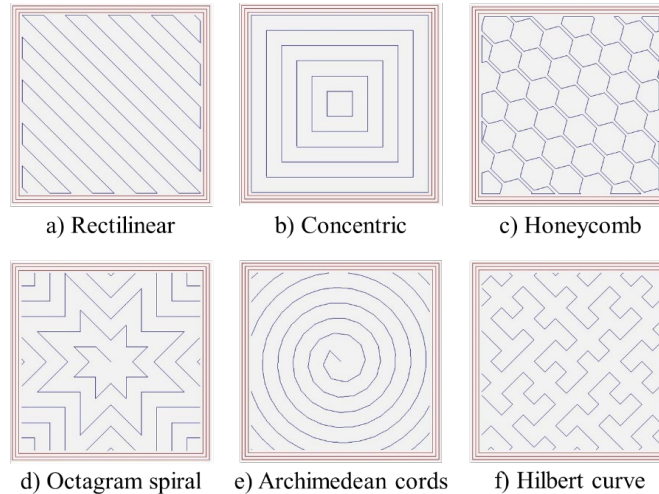


Figure 1. Six types of low density infill patterns.

Furthermore, Ćwikła et. al. [16] and Baich, Manogharan and Marie [17] stated that honeycomb infill pattern offered the highest tensile strength compared to other patterns. On the contrary, Khan et. al. [18] and Khan et. al. [19] mentioned that rectilinear infill pattern could provide a higher tensile strength compared to honeycomb and concentric infill patterns. Despite such confusion, even though there are more than six infill patterns available, the most popular patterns that were being studied in 3D printing were only rectilinear [20] and honeycomb [15] infill patterns. As consequences, there are very little information on rarely used infill patterns such as Hilbert curve, Archimedean cord and octagram spiral. In addition, to the authors' knowledge, there are no study that investigate and compares the tensile strength and other mechanical properties of all six infill patterns. To date, investigations done previously only addressed two or three commonly used infill patterns.

In this study, using polylactic acid (PLA) polymer as printing material, all six infill patterns have been investigated and compared to each other in term of their tensile properties. Then, based on these tensile strength and strain values, the optimum selection of infill patterns has been suggested so that the 3D printed parts can be used at its optimum function in various products innovation.

METHODOLOGY

Specimen Modelling

In order to study the influence of infill patterns to the tensile properties of 3D printed parts, the specimens were designed based on ASTM D638 Type III standards [21], as shown in Figure 2. The value of gage length L_0 , width of narrow section W , and thickness T were 50, 19, and 9.6 mm, respectively. The resulted volume is 34943.69 mm³. The 3D model was then exported in Standard Triangulation Language (STL) file format, which then further processed by a slicing software to implement various low density infill patterns, as shown in Figure 3. After that, the G-code files for each 3D model with specific infill pattern were generated by the slicing software. The G-code files, which translated the 3D design into position coordinates, were then used in an FFF 3D printer to fabricate the specimens layer by layer.

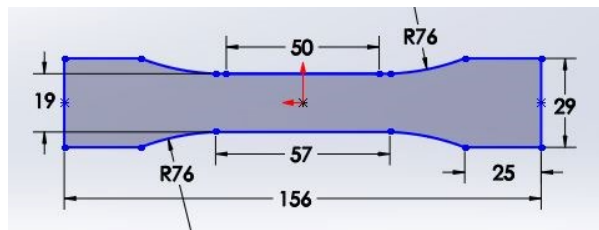


Figure 2. CAD model of ASTM D638 specimen (all dimension in mm).

3D Printing Setup and Fabrication

An open-source desktop FFF 3D printer with nozzle size of 0.4 mm and 300 x 300 mm heated bed were used to fabricate all the specimens. The constant values of main characteristics parameters are shown in Table 1. All the fabrication processes had been conducted in a controlled environment at room temperature to avoid a sudden change of temperature, which could cause common failure in 3D printed parts such as warping. In order to increase the accuracy of the results, ten specimens had been prepared for each infill pattern. In addition, ten specimens with solid infill (100% infill density) had also been prepared to be used for validation purpose. A total of 70 specimens had been fabricated. The material used was polylactic acid (PLA) polymer, which is a biodegradable thermoplastic obtained from natural lactic acid sources such as sugar feedstock [22]. PLA filament with diameter of 1.75 mm had been used as feeder material to the 3D printer extruder. Once all the specimens had been fabricated, the weight of each specimen was measured using weight scale and recorded prior to tensile testing.

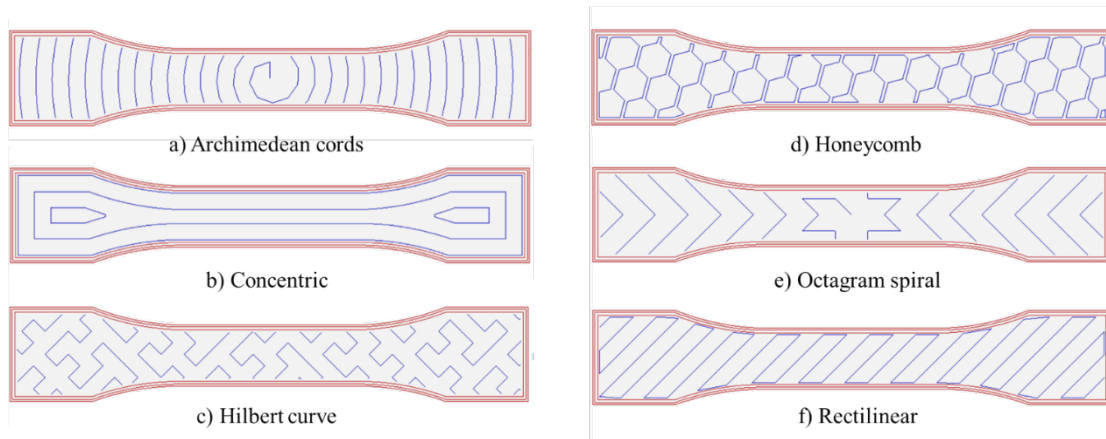


Figure 3. ASTM D638 specimens with implemented various infill patterns from (a) to (f).

Table 1. Constant values of main characteristic parameters.

Parameters (unit)	Value
Layer height (mm)	0.2
Vertical shell perimeters	4
Horizontal shell top/bottom layers	3
Infill pattern top/bottom layers	Rectilinear
Infill density (%)	20
Infill angle (°)	45
Nozzle temperature (°C)	210
Bed temperature (°C)	60

Tensile Testing

Tensile tests were conducted based on ASTM D638 standards using a 50 kN double column universal testing machine (UTM) at stroke speed of 5 mm/min. Calibration of the machine was done prior to the tensile testing. Since the UTM was directly connected to a computer, all measurements were synced and recorded automatically. Applied load F and resultant length L for all the specimens obtained from the tests were used in determining the values of tensile stress σ and strain ϵ , which are given by [21]:

$$\sigma = \frac{F}{A} = \frac{F}{W \times T} \tag{1}$$

$$\epsilon = \frac{L - L_0}{L_0} \times 100 \tag{2}$$

Here, A is the initial cross sectional area of the specimen, which is equal to 182.4 mm² while L_0 is the gage length of the specimen, which is 50 mm.

RESULTS AND DISCUSSION

Specimen Validation

In order to validate the experimental results, tensile strength of a solid specimen with 100% density obtained by tensile testing had been compared with previous experimental works by Farbman and McCoy [23] and Harpool [24]. As shown in Figure 4, the tensile strength obtained through experiment and previous literatures [23, 24] are 49.01, 46.18 and 42.92 MPa, respectively. In percentage comparison, the discrepancies between current study and previous studies are 6.1% and 12.4%, respectively. Such discrepancies are expected since the printing parameters are slightly different. Nevertheless,

such small discrepancies clearly indicated that the current method and results are appropriate to be carried out for all infill patterns.

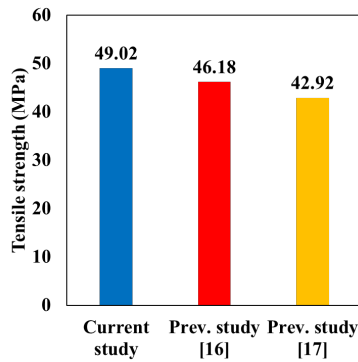


Figure 4. Comparison of tensile strength acquired through experiments in current study and previous literatures [23, 24].

Stress-strain Curve

Figure 5 shows the typical stress-strain curves of all six infill patterns, which are Archimedean chords (Arc.C), concentric (Conc), Hilbert curve (Hil.C), honeycomb (Hon.C), octagram spiral (Oct.S), and rectilinear (Rect). It can be observed that there is no clear linear elastic region at the initial stage of the curves since PLA thermoplastic is known to have a small value of Young’s modulus (3.4-3.6 GPa). Instead, a long strain hardening region can be observed where the plastic deformation continuously occurred until it reached the ultimate tensile strength. Apparently, the curve of all infill patterns showed that breaking occurred immediately after the ultimate tensile strength was achieved. Such behavior indicates a low ductility of the PLA thermoplastics at room temperature regardless of infill patterns.

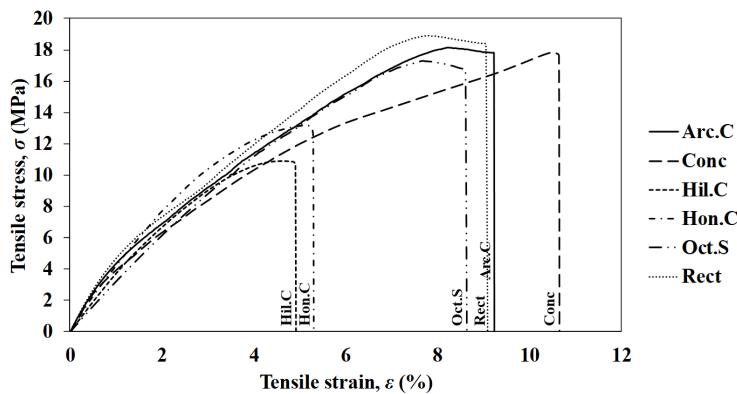


Figure 5. Typical stress-strain curves for all six infill patterns.

Tensile Strength

Table 2 shows the averaged values of main tensile strength properties of 20% infill (low density) 3D printed specimens having various infill patterns including solid specimen. Such comparison with solid is essential to provide a comprehensive relative difference among all infill patterns. In addition, the average weight and specific tensile strength (tensile strength per unit density) of each infill patterns are also included in Table 2. Since the implementation of infill patterns is intended for mass reduction, evaluation and comparison in term of specific tensile strength could serve as a normalized indicator to fairly evaluate the performance of each infill patterns across all tensile characteristics, including tensile strength and strain.

Figure 6 shows the ultimate tensile strength of each infill patterns and its corresponding weight. The value of tensile strength represents the bearable maximum stress. It can be observed that specimen with rectilinear infill pattern has the highest tensile strength of 18.90 MPa while Hilbert curve has the lowest value at 10.90 MPa. The error bars represent the standard deviation of measured tensile strength, where 68% of the measurements fell within that range. Small standard deviations can be seen for all infill patterns, which indicate a high repeatability and consistency. In comparison with solid specimens, the weight of all infill patterns has significantly reduced by approximately 50%. As a trade-off of such mass reduction, no infill pattern has a tensile strength value more than 40% of solid. Such fact indicates that by introducing infill patterns at low density (20%) to 3D printed parts, a major mass reduction could be achieved in an exchange of lower tensile strength.

Table 2. Averaged values of main tensile strength properties for various infill patterns.

Infill pattern	Tensile strength, σ (MPa)	Std. dev.	σ compare to solid (%)	Weight (g)	Density $\times 10^{-3}$ (g/mm ³)	Specific $\sigma \times 10^3$ (MPa·mm ³ /g)
Solid (100% infill)	49.01	1.774	100.0	43.50	1.245	39.37
Rectilinear	18.90	0.657	38.57	20.04	0.574	32.96
Concentric	17.93	1.224	36.57	20.02	0.573	31.28
Honeycomb	13.64	0.545	27.84	21.65	0.619	22.03
Octagram spiral	17.05	0.542	34.79	19.24	0.551	30.98
Archimedean cords	18.28	1.288	37.29	19.22	0.550	33.23
Hilbert curve	10.90	0.586	22.25	19.24	0.551	19.80

Moreover, based on the value of tensile strength in Table 2, a trend from the highest to the lowest could be obtained. As shown in Figure 7, rectilinear is the highest, followed by Archimedean chords, concentric, octagram spiral, honeycomb, and lastly Hilbert curve. Similar trend has also been found by Khan et. al. [18]. However, the previous study [18] was limited only to three infill patterns which are rectilinear, concentric, and honeycomb. On top of such patterns, this study provides a new information on the trend of rarely investigated such as Archimedean cords, octagram spiral, and Hilbert curves. It can be observed in Figure 7 that Archimedean cords lies between rectilinear and concentric, while octagram spiral lies between concentric and honeycomb. It is also noted that Hilbert curve is at the last position of the trend, after honeycomb.

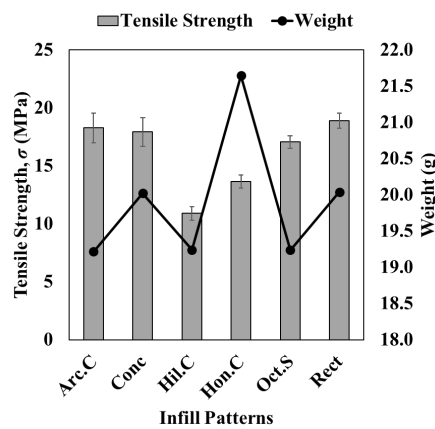


Figure 6. Tensile strength of each infill patterns and its corresponding weight.

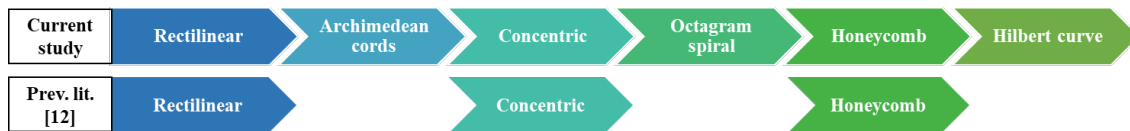


Figure 7. Trend of tensile strength from the strongest to the weakest.

Furthermore, at low infill density, rectilinear infill pattern is the strongest owing to its internal mesostructure, where it has many intersections of two layers of contrasting directions, which lead to a high stress tolerance with minimum materials. On the other hand, since honeycomb infill pattern consisted of hexagonal geometries adjacent to each other, it resulted in a high usage of material that is concentrated at the neighboring borders with a lot of free spaces in between. As consequences, at low density infill, honeycomb infill pattern has more weight but less tensile strength. Utilizing such low density honeycomb infill pattern in products' fabrication is a wastage of material. In addition, the fact that rectilinear has a higher tensile strength compared to honeycomb infill pattern at low infill density is in line with those reported by Khan et. al. [19].

As for hardly investigated infill patterns such as Archimedean cords, octagram spiral, and Hilbert curve, it has become apparent that these infill patterns have less weight compared to the others, which indicate that these patterns are very effective for mass reduction of 3D printed parts. The weights of these patterns only deviated approximately 0.1% among each other. However, Archimedean cords showed the best potential in mass reduction since it provided relatively high tensile strength of 18.28 MPa while at the same time had the least weight of 19.22 g.

Strain Properties

Table 3 shows the averaged values of strain properties of 20% infill (low density) 3D printed specimens having various infill patterns including solid specimen. In this study, the properties of solid specimen have been used as reference values in order to understand the differences among all infill patterns. In addition, the average weight and specific strain (strain per unit density) of each infill patterns are also included in Table 3. As been mentioned before, the purpose of using the

value of specific strain in comparing the performance of infill patterns is to have a fair evaluation across all types of infill patterns.

Table 3. Averaged values of main strain properties for various infill patterns.

Infill pattern	Strain, ϵ (%)	Std. dev.	ϵ compare to solid (%)	Weight (g)	Density $\times 10^{-3}$ (g/mm ³)	Specific $\epsilon \times 10^3$ (%·mm ³ /g)
Solid (100% infill)	10.17	0.467	100.0	43.50	1.245	8.17
Rectilinear	7.96	0.677	78.22	20.04	0.574	13.87
Concentric	10.43	1.380	102.6	20.02	0.573	18.21
Honeycomb	5.58	0.382	54.84	21.65	0.619	9.00
Octagram spiral	8.54	0.770	83.94	19.24	0.551	15.51
Archimedean cords	7.93	0.864	77.99	19.22	0.550	14.42
Hilbert curve	4.59	0.304	45.14	19.24	0.551	8.34

The strain of each infill patterns, along with its corresponding weight, are shown in Figure 8. These strains indirectly represent the elongation tolerance of each infill patterns towards applied stress before failure. In other words, a higher strain value allows a higher deformation before the specimens break apart. It can be observed in Figure 8 that concentric infill pattern has the highest strain value of 10.43% while Hilbert curves being the lowest with value of 4.59%. It is also noted that the values of standard deviation are small for all infill patterns, which indicate a strong consistency. Moreover, such significant different between the highest and the lowest strain values are accompanied by a mere 0.78 g difference in weight. From these results, it can be expected that in products innovation that involve large material's mass and volume, the selection of infill patterns will become extraordinarily important since a slight increase in mass will cause a significant change in strain of the products.

Furthermore, it can be observed in Table 3 that concentric infill pattern has a higher strain value compared to solid, with an extra of 2.58%. Such interesting result provides evidence that the introduction of infill patterns in the fabrication of 3D printed parts is very useful, since it can reduce the amount of material used while at the same time preserving the strain properties. Not to mention that Hilbert curve has the least strain that equivalent to only 45.14% of solid. In other words, it can be said that by introducing infill patterns into the 3D printed parts, the maximum reduction in strain was only 54.84%. Such reduction in strain seems to be reasonable in an exchange of 55% reduction in mass, which is obtained by comparing the weight of solid specimen and Hilbert curve infill pattern.

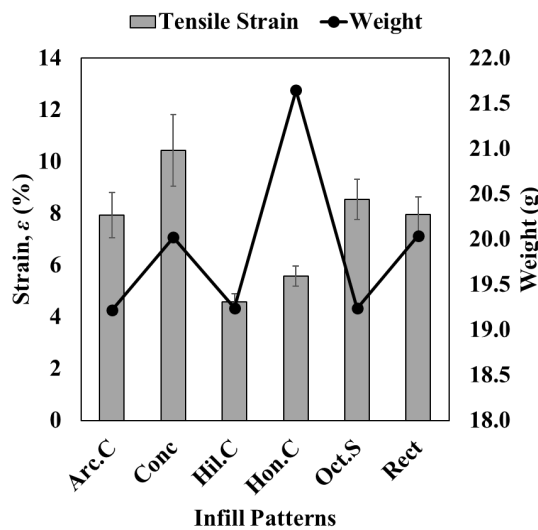


Figure 8. Strain of each infill patterns and its corresponding weight.



Figure 9. Trend of strain from the strongest to the weakest.

Based on Figure 8, by rearranging the infill patterns with strain value from the highest to the lowest, a trend of strain could be obtained starting with concentric, followed by octagram spiral, rectilinear, Archimedean cords, honeycomb, and lastly Hilbert curve. The fact that concentric infill pattern has the highest strain value is in agreement with previous study [18]. The comparison between the strain trend from current study and previous one is shown in Figure 9. Such trend of

strain is a very important information in products innovation that needs to balance between strain and mass. Despite the slight difference in the trend, current study provides a new insight on the strain's trend of six infill patterns, including those that are irregularly studied such as octagram spiral, Archimedean chords and Hilbert curve.

The novelty of current study lies in the comprehensive understanding about the above mentioned irregularly studied infill patterns, namely octagram spiral, Archimedean chords and Hilbert curve. Since these infill patterns have never been studied, there is no report on actual implementation of these infill patterns either by industries or researchers. Nevertheless, as shown in Table 2 and 3, it has become apparent that, in term of tensile strength, octagram spiral and Archimedean chords are good alternatives to commonly used rectilinear and honeycomb patterns, since they are stronger compared to honeycomb while slightly weaker (3.3~9.8%) than that of rectilinear. Furthermore, in term of strain, it is better to use octagram spiral due to its higher deformability before break compared to rectilinear (12.1% higher) and honeycomb (50.3% higher). Regardless of strength or strain, Hilbert curve infill pattern should be avoided since it is the weakest among all.

In addition, to understand further about mass reduction and its relationship with tensile strength as well as strain, the specific tensile strength and strain of each infill patterns were shown in Figure 10. It is observed that Archimedean cords was the best potential infill pattern in mass reduction since it provided the highest specific tensile strength, with the value of $33.23 \times 10^3 \text{ MPa}\cdot\text{mm}^3/\text{g}$, higher than that of rectilinear. However, when considering both tensile strength and strain, it can be concluded that concentric infill pattern is the best candidate to be utilized to produce not only a lightweight 3D printed parts but also have a better elongation before failure with specific strain of $18.21 \times 10^3 \text{ \%}\cdot\text{mm}^3/\text{g}$. This is due to the fact that concentric infill pattern offered the highest value of specific strain and relatively high value of specific tensile strength. Such properties of concentric infill pattern are owing to its continuous circumvoluted structure of concentrated center with erased internal intersecting geometry that can tolerate a high deformation. On the other hand, even though Hilbert curve is among the infill patterns with less weight, it is better to avoid such infill pattern due to its poor performance in term of both specific tensile strength and strain. Nevertheless, it is interesting to observed that Hilbert curve infill pattern, being the infill pattern with the lowest value of strain, still outperformed the solid one in term of specific strain. It is also very intriguing to observe that infill pattern that offered high tensile strength do not necessarily has a high strain value, such as rectilinear.

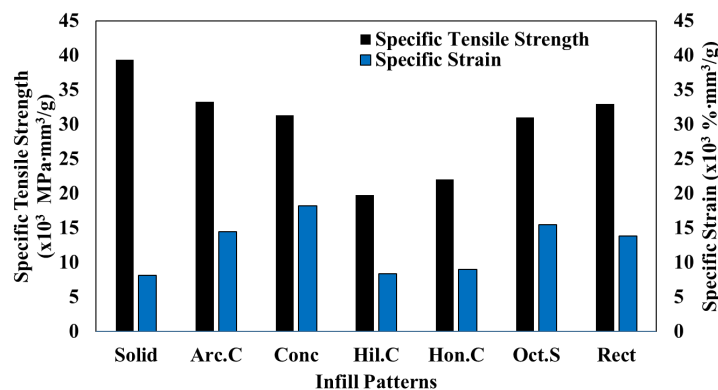


Figure 10. Comparison between tensile strength per unit mass and strain per unit mass for each infill pattern.

CONCLUSION

In conclusion, the tensile characteristics of six different low density (20%) infill patterns for mass reduction of 3D printed PLA parts have been studied and compared side-by-side. It is found that Archimedean cords infill pattern with the highest specific tensile strength of $33.23 \times 10^3 \text{ MPa}\cdot\text{mm}^3/\text{g}$ is the most suitable pattern to be used in mass reduction of 3D printed parts that can withstand a high tensile force. It is also found that concentric infill pattern having the highest specific strain of $18.21 \times 10^3 \text{ \%}\cdot\text{mm}^3/\text{g}$ is favorable for a lightweight 3D printed part that requires a higher elongation before break. From the tensile characteristics, Hilbert curve is the least suggested pattern to be used since it has the least values of specific tensile strength and strain, which are $19.80 \times 10^3 \text{ MPa}\cdot\text{mm}^3/\text{g}$ and $8.34 \text{ \%}\cdot\text{mm}^3/\text{g}$, respectively. Most importantly, the trend of tensile strength and strain for all six patterns also have been brought to light, especially for rarely investigated infill patterns such as Archimedean chords, octagram spiral and Hilbert curve. In addition, finite element analyses are desirable to be conducted in the future in order to comprehensively understand the stress distribution and failure points inside the specimens having various infill patterns, especially for Hilbert curve, Archimedean cords and octagram spiral infill patterns.

ACKNOWLEDGEMENT

Financial aid under Short Term Research Grant (STRG: str19015) and facilities provided by Universiti Kuala Lumpur (UniKL) is acknowledged and very much appreciated.

REFERENCES

- [1] Wang X, Jiang M, Zhou Z, Gou J, Hui D. 3D printing of polymer matrix composites: A review and prospective. *Composites Part B: Engineering*, 2017; 110: 442-458.
- [2] Nachtane M, Tarfaoui M, El Moumen A, Saifaoui D, Benyahia H. Design and hydrodynamic performance of a horizontal axis hydrokinetic turbine. *International Journal of Automotive and Mechanical Engineering*, 2019; 16(2): 6453-6469.
- [3] Nithesh N, Prajwal S. Effect of splitters in recirculation channels on performance of turbocharger compressors used in gasoline engines-a CFD study. *International Journal of Automotive and Mechanical Engineering*, 2019; 16(1): 6214-6229.
- [4] Saari M, Nadzri N, Halil A, Ishak M, Sakai K, Kiwa T, Tsukada K. Design of Eddy current testing probe for surface defect evaluation. *International Journal of Automotive and Mechanical Engineering*, 2019; 16(1): 6357-6367.
- [5] Vallhagen J, Madrid J, Söderberg R, Wärmeffjord K. An approach for producibility and DFM-methodology in aerospace engine component development. *Procedia CIRP*, 2013; 11: 151-156.
- [6] Huang SH, Liu P, Mokasdar A, Hou L. Additive manufacturing and its societal impact: A literature review. *The International Journal of Advanced Manufacturing Technology*, 2012; 67(5-8): 1191-1203.
- [7] Matias E, Rao B. 3D printing: On its historical evolution and the implications for business. In: 2015 Portland International Conference on Management of Engineering and Technology (PICMET), pp. 551-558, 2015.
- [8] Petrovic V, Vicente Haro Gonzalez J, Jordá Ferrando O, Delgado Gordillo J, Ramón Blasco Puchades J, Portolés Griñan L. Additive layered manufacturing: Sectors of industrial application shown through case studies. *International Journal of Production Research*, 2010; 49(4): 1061-1079.
- [9] Ramesh M, Panneerselvam K. PLA-based material design and investigation of its properties by FDM. In: *Advances in additive manufacturing and joining*, 2020; pp. 229-241.
- [10] Kiendl J, Gao C. Controlling toughness and strength of fdm 3D-printed PLA components through the raster layup. *Composites Part B: Engineering*, 2020; 180.
- [11] Wu J. Study on optimization of 3D printing parameters. *IOP Conference Series: Materials Science and Engineering*, 2018; 392: 062050.
- [12] Sood AK, Ohdar RK, Mahapatra SS. Experimental investigation and empirical modelling of FDM process for compressive strength improvement. *Journal of Advanced Research*, 2012; 3(1): 81-90.
- [13] Moscato S, Bahr R, Le T, Pasian M, Bozzi M, Perregri L, Tentzeris MM. Infill-dependent 3D-printed material based on Ninjaflex filament for antenna applications. *IEEE Antennas and Wireless Propagation Letters*, 2016; 15: 1506-1509.
- [14] de Vos M, Tudor J, Torah R. Effect of infill patterns on print quality of dispenser-printed electronic ink. *Electronics Letters*, 2015; 51(15): 1186-1187.
- [15] Fernandez-Vicente M, Calle W, Ferrandiz S, Conejero A. Effect of infill parameters on tensile mechanical behavior in desktop 3D printing. *3D Printing and Additive Manufacturing*, 2016; 3(3): 183-192.
- [16] Ćwikła G, Grabowik C, Kalinowski K, Paprocka I, Ociepka P. The influence of printing parameters on selected mechanical properties of FDM/FFF 3D-printed parts. *IOP Conference Series: Materials Science and Engineering*, 2017; 227: 012033.
- [17] Baich L, Manogharan G, Marie H. Study of infill print design on production cost-time of 3D printed ABS parts. *International Journal of Rapid Manufacturing*, 2015; 5(3/4): 308.
- [18] Khan SA, Siddiqui BA, Fahad M, Khan MA. Evaluation of the effect of infill pattern on mechanical strength of additively manufactured specimen. *Materials Science Forum*, 2017; 887: 128-132.
- [19] Khan SF, Zakaria H, Chong YL, Saad MAM, Basaruddin K. Effect of infill on tensile and flexural strength of 3D printed PLA parts. *IOP Conference Series: Materials Science and Engineering*, 2018; 429: 012101.
- [20] Yao T, Ye J, Deng Z, Zhang K, Ma Y, Ouyang H. Tensile failure strength and separation angle of fdm 3D printing pla material: Experimental and theoretical analyses. *Composites Part B: Engineering*, 2020; 188.
- [21] Gooch JW. Astm d638. In: *Encyclopedic dictionary of polymers*, 2011; pp. 51.
- [22] Lunt J. Large-scale production, properties and commercial applications of polylactic acid polymers. *Polymer Degradation and Stability*, 1998; 59(1-3): 145-152.
- [23] Farbman D, McCoy C. Materials testing of 3D printed ABS and PLA samples to guide mechanical design. In: *ASME 2016 11th International Manufacturing Science and Engineering Conference, Volume 2: Materials; Biomanufacturing; Properties, Applications and Systems; Sustainable Manufacturing*, Virginia, USA, pp. V002T001A015; June 27–July 1, 2016.
- [24] Harpool TD. Observing the effect of infill shapes on the tensile characteristics of 3D printed plastic parts. *Wichita State University*, 2016.